

Atmospheric Environment 35 (2001) 1627-1637

## ATMOSPHERIC ENVIRONMENT

www.elsevier.com/locate/atmosenv

# Two-level time-marching scheme using splines for solving the advection equation

### Khoi Nguyen, Donald Dabdub\*

Department of Mechanical and Aerospace Engineering, University of California at Irvine, Irvine, CA 92697-3975, USA

Received 17 August 2000; accepted 28 August 2000

#### Abstract

A new numerical algorithm using quintic splines is developed and analyzed: quintic spline Taylor-series expansion (QSTSE). QSTSE is an Eulerian flux-based scheme that uses quintic splines to compute space derivatives and Taylor series expansion to march in time. The new scheme is strictly mass conservative and positive definite while maintaining high peak retention. The new algorithm is compared against accurate space derivatives (ASD), Galerkin finite element techniques, and the Bott scheme. The cases presented include classical rotational fields, deformative fields, as well as a full-scale aerosol model. Research shows that QSTSE presents significant improvements in speed and oscillation suppression against ASD. Furthermore, QSTSE predicts some of the most accurate results among the schemes tested. © 2001 Elsevier Science Ltd. All rights reserved.

Keywords: Hyperbolic systems; Air quality models; Eulerian methods; Taylor expansion; Finite differences

### 1. Introduction

The classical advection equation often appears in development of air quality models. The one-dimensional form of the advection equation is given as

$$\frac{\partial c}{\partial t} + \frac{\partial uc}{\partial x} = 0,\tag{1}$$

where u is the wind velocity and c is the concentration. The extension to higher dimensions in air quality models is usually performed through operator splitting (Yanenko, 1971), which is widely used in air quality modeling (Harley et al., 1993). It is well known that the numerical solution to Eq. (1) leads to dispersions and oscillations (Oran and Boris, 1987). To address this problem, the development of various advection schemes has been a continuing effort. A review of such schemes as they apply to air quality models is found in Rood (1987),

Chock (1985, 1991), Chock and Dunker (1983), and Dabdub and Seinfeld (1994).

There are numerous techniques used to solve the advection equation. Some of the popular techniques are Eulerian finite differences, flux-based schemes (Bott, 1989), Lagrangian characteristics (Augenbaum, 1984) and semi-Lagrangian methods (Purnell, 1976). Each method has merits in certain cases and problems in others. For example, Lagrangian methods are ideal for advection processes but incur difficulties since trajectories scatter points non-uniformly. This problem leads to inefficiencies and inaccuracies since data fields in air quality models are usually given at uniform grid points. Eulerian finite differences are attractive due to their simplicity, flux-based schemes are tailored to be conservative, while semi-Lagrangian methods provide higher stability and thus, larger time steps (Bermejo and Staniforth, 1992). However, semi-Lagrangian methods tend not to obey mass conservation and require additional mass adjustments (Huang, 1996).

This paper presents the development and analysis of QSTSE, a new Eulerian method to solve the advection equation. The formulation of the algorithm is presented in Section 2. The performance tests of the algorithm are

<sup>\*</sup>Corresponding author. Tel.: +1-949-824-6126; fax: +1-949-824-8585.

E-mail addresses: khnguy@eng.uci.edu (K. Nguyen), ddab-dub@uci.edu (D. Dabdub).

presented in Section 3. The performances are gauged by classical advection tests as well as a three-dimensional atmospheric aerosol dynamic model.

### 2. Algorithm description

### 2.1. The non-flux quintic spline with Taylor-series expansion (NFQSTSE) algorithm

Classical finite difference schemes such as second-order central differences can be derived from interpolation of data. In particular, second-order central differences can be attained from interpolating piece-wise quadratic polynomials. Similarly, fourth-order five-point finite differences can be derived from a quartic polynomial fit. The use of splines as an interpolator has become increasingly popular. Spline interpolators are viable alternatives to Lagrange-polynomial interpolators, thus, spline derivative schemes provide competitive alternatives to classical Taylor finite difference schemes.

In quintic spline interpolation schemes, piece-wise quintic polynomials are fitted to data points requiring continuous fourth derivatives globally. Consider a uniform grid in x with N points, a quintic spline,  $S_j(x)$  on the grid interval  $(x_i, x_{j+1})$  that interpolates nodal values  $a_j$  is

$$S_j(x) = a_j + b_j(x - x_j) + c_j(x - x_j)^2 + d_j(x - x_j)^3 + e_j(x - x_j)^4 + f_j(x - x_j)^5,$$
(2)

where  $1 \le j \le N-1$  and  $b_j$ ,  $c_j$ ,  $d_j$ ,  $e_j$ ,  $f_j$  are the linear, quadratic, cubic, quartic and quintic coefficients of the spline, respectively. Setting  $h = x_{j+1} - x_j$  and requiring continuous fourth derivatives, yields the following system of equations:

$$a_{i+1} = a_i + b_i h + c_i h^2 + d_i h^3 + e_i h^4 + f_i h^5,$$
 (3)

$$b_{i+1} = b_i + 2c_i h + 3d_i h^2 + 4e_i h^3 + 5f_i h^4, \tag{4}$$

$$2c_{i+1} = 2c_i + 6d_ih + 12e_ih^2 + 20f_ih^3, (5)$$

$$6d_{i+1} = 6d_i + 24e_i h + 60f_i h^2, (6)$$

$$24e_{i+1} = 24e_i + 120f_i h. (7)$$

An efficient solution to these equations is found in De Boor (1978). Eq. (1) is reduced to an ordinary differential equation in time with the coefficients of the spline, which are proportional to the derivatives at nodal points. To advance in time, a time-marching scheme (e.g. Runge-Kutta), a Taylor series in time, or even an exponential solver can be used. In this paper, a Taylor series in time is used due to its computational efficiencies. If a truncated Taylor approximation in time is applied, a fourth-order

expansion or less should be used because the fifth derivative is generally discontinuous with quintic splines. Consider a fourth-order Taylor expansion in time expressed as follows:

$$c(t + \Delta t) \cong c(t) + \sum_{i=1}^{4} \frac{\partial^{i} c}{\partial t^{i}} \frac{\Delta t^{i}}{i!} + \text{h.o.t.},$$
 (8)

The derivative in time can be substituted by the derivative in space via differentiating Eq. (1). Assuming that u is time independent on the interval, dt (which is often applied in air quality models as described by Harley et al., 1993), the second derivative of c with respect to t can be expressed as

$$\frac{\partial^2 c}{\partial t^2} = \frac{\partial}{\partial t} \frac{\partial c}{\partial t} = -\frac{\partial}{\partial x} \frac{\partial uc}{\partial t} = \frac{\partial}{\partial x} \left( u \frac{\partial uc}{\partial x} \right). \tag{9}$$

Higher-order terms are retrieved using the same principle and are given as

$$\frac{\partial^3 c}{\partial t^3} = -\left(\frac{\partial u}{\partial x}\right)^2 \frac{\partial uc}{\partial x} - 3u \frac{\partial u}{\partial x} \frac{\partial^2 uc}{\partial x^2} + u\left(\frac{\partial uc}{\partial x} \frac{\partial^2 u}{\partial x^2} - u \frac{\partial^3 uc}{\partial x^3}\right),\tag{10}$$

$$\frac{\partial^{4}c}{\partial t^{4}} = \left(\frac{\partial u}{\partial x}\right)^{3} \frac{\partial uc}{\partial x} + 7u \left(\frac{\partial u}{\partial x}\right)^{2} \frac{\partial^{2}uc}{\partial x^{2}} + 2u \frac{\partial u}{\partial x} \left(2 \frac{\partial uc}{\partial x} \frac{\partial^{2}u}{\partial x^{2}}\right) + 3u \frac{\partial^{2}uc}{\partial x^{2}}\right) + u^{2} \left(4 \frac{\partial^{2}u}{\partial x^{2}} \frac{\partial^{2}uc}{\partial x^{2}} + \frac{\partial uc}{\partial x} \frac{\partial^{3}u}{\partial x^{3}} + u \frac{\partial^{4}uc}{\partial x^{4}}\right). \tag{11}$$

With a fourth-order Taylor expansion, it is possible to march in time with high accuracy and efficiency since derivatives of uc and u with respect to x are readily available in quintic splines. The memory requirement of this time scheme is minimal since it is a two-level time-marching scheme or a forward-time technique.

The method described so far, shall be called NFQSTSE, the non-flux quintic spline Taylor-series Expansion. The stability and eigenvalue analysis of this method is detailed in the appendix.

NFQSTSE is integrally mass conservative. Integral mass conservation is proven simply by integrating Eq. (8) over the entire domain and using splines with periodic end conditions. Periodic splines are commonly used in various disciplines, where the derivatives at endpoints are equal (Spath, 1995; Dubeau and Savoie, 1983; Spath and Meier, 1988). Starting with Eq. (8)

$$c(x,t+\Delta t) = c(x,t) + \frac{\partial c}{\partial t} \Delta t + \frac{\partial^2 c}{2! \partial t^2} \Delta t^2 + \frac{\partial^3 c}{3! \partial t^3} \Delta t^3 + \frac{\partial^4 c}{4! \partial t^4} \Delta t^4$$
(12)

and applying Eq. (1) yields

$$c(x,t + \Delta t) = c(x,t) - \frac{\partial uc}{\partial x} \Delta t + \frac{\partial}{\partial x} \left[ u \frac{\partial uc}{\partial x} \right] \frac{\Delta t^2}{2!}$$
$$- \frac{\partial}{\partial x} \left[ u \frac{\partial}{\partial x} \left[ u \frac{\partial uc}{\partial x} \right] \right] \frac{\Delta t^3}{3!}$$
$$+ \frac{\partial}{\partial x} \left[ u \frac{\partial}{\partial x} \left[ u \frac{\partial}{\partial x} \left[ u \frac{\partial uc}{\partial x} \right] \right] \frac{\Delta t^4}{4!}. \tag{13}$$

Integrating both side over the domain would produce a mass balance.

$$\int_{x_0}^{x_f} c(x, t + \Delta t) dx = \int_{x_0}^{x_f} c(x, t) dx - \int_{x_0}^{x_f} \frac{\partial uc}{\partial x} \Delta t$$

$$+ \frac{\partial}{\partial x} \left[ u \frac{\partial uc}{\partial x} \right] \frac{\Delta t^2}{2!}$$

$$- \frac{\partial}{\partial x} \left[ u \frac{\partial}{\partial x} \left[ u \frac{\partial uc}{\partial x} \right] \right] \frac{\Delta t^3}{3!}$$

$$+ \frac{\partial}{\partial x} \left[ u \frac{\partial}{\partial x} \left[ u \frac{\partial}{\partial x} \left[ u \frac{\partial uc}{\partial x} \right] \right] \right] \frac{\Delta t^4}{4!} dx,$$
(14)

where  $[x_0, x_f]$  is the interval of the domain. If the expressions inside the integral is continuous or defined uniquely over the domain and with specified periodic conditions,  $uc(x) \equiv u(x)c(x), uc(x_0) = uc(x_f), \ \partial^i uc(x_0)/\partial x^i = \partial^i uc(x_f)/\partial x^i$  for  $i = 1 \dots 4$  then Eq. (14) reduces to the conservation of mass in integral form

$$\int_{x_0}^{x_f} c(x, t + \Delta t) \, \mathrm{d}x = \int_{x_0}^{x_f} c(x, t) \, \mathrm{d}x. \tag{15}$$

### 2.2. Quintic spline with Taylor-series expansion (QSTSE) algorithm

QSTSE is a discretely mass conservative flux-based scheme. It is derived from NFQSTSE by similar fashion as the proof of NFQSTSE's integral mass conservation. If Eq. (8) is evaluated at cell centers, the integration over each cell yields a flux system,

$$\int_{x_j}^{x_{j+1}} c(x, t + \Delta t) dx = \int_{x_j}^{x_{j+1}} c(x, t) dx + \Delta t \int_{x_j}^{x_{j+1}} \frac{\partial c}{\partial t} + \frac{\partial^2 c}{2! \partial t^2} \Delta t + \frac{\partial^3 c}{3! \partial t^3} \Delta t^2 + \frac{\partial^4 c}{4! \partial t^4} \Delta t^3 dx,$$
 (16)

where  $x_j$  and  $x_{j+1}$  is the position of the cell's left and right boundaries, respectively. Integrating Eq. (16) yields,

$$C_i^{n+1} \Delta x = C_i^n \Delta x + \Delta t (F_{i+1} - F_i). \tag{17}$$

Here,  $C_j^{n+1}$ ,  $C_j^n$ ,  $F_{j+1}$  and  $F_j$  are the average concentration at time step n+1, average concentration at time step n, flux from the right boundary and flux from the left boundary respectively. The sum of Eq. (17) over j is the statement of discrete mass conservation. Depending on how the integration of Eq. (16) is performed, different discretely conservative schemes arise. In particular, if the integration is performed analytically, the flux is given as

$$F_{j} = uc(x_{j}) + \left[u(x_{j})\frac{\partial uc(x_{j})}{\partial x}\right]\frac{\Delta t}{2!} + \left[u(x_{j})\frac{\partial}{\partial x}\left[u(x_{j})\frac{\partial uc(x_{j})}{\partial x}\right]\right]\frac{\Delta t^{2}}{3!} + \left[u(x_{j})\frac{\partial}{\partial x}\left[u(x_{j})\frac{\partial}{\partial x}\left[u(x_{j})\frac{\partial uc(x_{j})}{\partial x}\right]\right]\right]\frac{\Delta t^{3}}{4!}.$$
(18)

where the derivatives are evaluated by quintic splines. However, the performance of this method is diffusive compared to NFQSTSE described in Section 2.1. To remedy this diffusive problem, QSTSE uses a histospline (area-preserving spline) to compute the integration (Schoenberg, 1983; Spath, 1995). By using a histospline, QSTSE maintains the high accuracy of NFQSTSE but is discretely mass conservative since it is a flux formulation.

QSTSE is positive definite. Namely, positive definiteness is maintained by flux limitation similar to that used by Bott (1989). If the total outflow is limited by how much mass is available. Mathematically that is given as

$$F_{j+1} \geqslant -\frac{\Delta x}{\Lambda t} C_j^n + F_j. \tag{19}$$

Splines are well suited for many interpolation problems like that in advection. In this paper, area preserving, periodic and natural splines are implemented. Many spline interpolators exist that are positive definite (Schmidt and Hess, 1988; Fischer et al., 1991), shape preserving (Costantini, 1988; McAllister et al., 1977), and monotonic (Costantini, 1986). These spline properties are ideal for flux-integrated semi-Lagrangian methods, but is not required in the approach developed here since the interpolation is performed on the flux and not the concentration.

### 3. Description of numerical tests

Test cases are chosen to gauge the performance of QSTSE under a variety of conditions. The rotating cosine hill in test I, as proposed by Pepper and Long (1978), provides fundamental requirements for advection schemes: peak retention. The cosine hill distribution is chosen since it represents typical profiles of high pollutant concentration while maintaining a stringent test case. In test II, a rugged concentration profile is advected

Table 1
Performance of various unfiltered schemes on the cosine hill test after two revolutions. MI, MC, MD, and ME are the minimum
concentration ratio, mass conservation ratio, mass distribution ratio, and maximum error ratio, respectively

Algorithm	Reference	Description	Peak	MI	MC	MD	ME	Rel. Time
GLK	Dabdub and Seinfeld (1994)	Fourth-order Taylor-Galerkin	91	- 0.14	0.999	0.999	0.283	1.0
ASD	Gazdag (1973)	Taylor expansion with Fourier derivatives	98	- 0.01	0.999	0.981	0.132	40.7
QSTSE	This work	Fourth-order Taylor expansion with quintic splines	101	- 0.01	1.000	0.998	0.021	5.8
NFQSTSE2	This work	Second-order Taylor expansion with quintic splines	104	- 0.18	1.002	1.073	0.341	5.2
NFCSTSE	This work	Second-order Taylor expansion with cubic splines	78	- 0.04	1.000	1.930	0.213	3.2
BOTT4	Bott (1988)	Nonlinear flux normalization flux scheme	77	- 0.10	1.000	1.125	0.237	2.3

to gauge the performance of QSTSE under stringent modulation. Conservation of mass under divergent flow fields is measured in test III where a sharp spike is advected through a velocity ramp. The flow of Smolar-kiewicz (1982) tests QSTSE under conditions that are massively deformative in test IV. Though this condition is more stringent than actual atmospheric conditions, it provides a good indicator of the scheme's ability to evolve correctly under a strongly deformative field. Test V gauges the behavior of the QSTSE under more realistic atmospheric conditions of the South Coast Air Basin of California. Test V implements QSTSE into a full three-dimensional grid-based air quality model, the CIT Airshed Model (Harley et al., 1993).

The schemes that are selected to be compared with QSTSE are summarized in Table 1. NFCSTSE is a Taylor expansion in time using a cubic spline and a second-order marching in time. NFQSTSE2 is similar to NFQSTSE but uses a second-order marching in time instead of a fourth order. GLK is chosen for its fast speed. ASD (Gazdag, 1973) is used for being most accurate beyond some 20 other solvers as presented by Chock (1991, 1985), Chock and Dunker (1983) and confirmed by Dabdub and Seinfeld (1994). Bott solvers present competitive accuracy, speed and mathematical conservation properties (Bott, 1989; Dhaniyala and Wexler, 1996).

Test I: Rotating cosine hill: The test consists of a  $33 \times 33$  uniform mesh with center at (17, 17) and a spacing of 1. The test is described as

$$\frac{\partial c}{\partial t} + \omega x \, \frac{\partial c}{\partial y} - \omega y \, \frac{\partial c}{\partial x} = 0,$$

where  $\omega$  is such that the cosine hill rotates two revolutions in  $7200\pi$  time units. The test has the following initial and boundary conditions

c = 10 on the boundary,

$$c(x,y) = \begin{cases} 45\left[1 + \cos(\frac{r\pi}{4})\right] + 10 & \text{if } r \leq 4, \\ 10 & \text{otherwise,} \end{cases}$$

where  $r = \sqrt{(x-7)^2 + (y-17)^2}$ . The time increment used in this test is  $30\pi$ , thus, requiring 240 time steps to complete two revolutions.

Test II: Rugged profile: Suitability of QSTSE with rugged concentration profile undergoing advection is tested here. Consider a one-dimensional grid with 33 points with space increments of 1.0. The advective wind field is a constant wind field with Courant number of 0.2. A rugged concentration profile with thin square waves of various distances apart is transported downwind. Mathematically, the case is given as

$$u(x) = 0.2 \tag{20}$$

with two initial conditions representing various spacings

$$c_i(x) = \begin{cases} 1 & \text{if } x = 2, 3, 4+i, 5+i, \\ 0 & \text{otherwise} \end{cases}$$

for i = 1 and i = 2. These initial conditions are advected downwind for 20 grid points or 100 time steps.

Test III: A ramp velocity profile: The following test is presented in Chock et al. (1996) and consist of a single spike advecting through a divergent field. Consider a grid of 33 points with the following initial condition given by:

$$c(x) = \begin{cases} 1 & \text{if } x = 5, \\ 0 & \text{otherwise} \end{cases}$$

with a velocity profile of

$$u(x) = \begin{cases} 0.1 & \text{if } x \le 10, \\ 0.1 + \frac{(x-10)}{50} & \text{if } 10 \le x \le 15, \\ 0.2 & \text{if } x \ge 15. \end{cases}$$

The test gauges QSTSE's mass conservation performance as it goes through the velocity ramp with a time step of 1 for 125 time steps.

Test IV: Deformative wind field: Consider a  $100 \times 100$  uniform grid in two dimensions with velocity profiles

$$u(x,y) = \frac{8\pi}{25} \sin\left(\frac{\pi x}{25}\right) \sin\left(\frac{\pi y}{25}\right)$$
 (21)

$$v(x,y) = \frac{8\pi}{25}\cos\left(\frac{\pi x}{25}\right)\cos\left(\frac{\pi y}{25}\right). \tag{22}$$

With initial conditions,

$$c(x, y) = \begin{cases} 100 - \frac{100r}{15} & \text{if } r \leq 15, \\ 0 & \text{otherwise,} \end{cases}$$

where  $r = \sqrt{(x-5)^2 + (y-50)^2}$ . The space increment is unity and the time increment,  $\Delta t = 0.7$ . The exact graphical solution to this test is presented by Staniforth et al. (1987) and the solution should be compared to the exact solution after short integration time (Bott, 1989).

Test V: Practical application: The final test is a full implementation in the CIT airshed model (Harley et al., 1993). The CIT model includes advection, diffusion, chemistry, deposition and emissions. The episode simulates 27 August 1987 for the South Coast Air Basin of California. The domain is irregular and has 5 layers in the vertical direction with 994 grid points in each layer. The spacing between each grid point in a layer is 5000 m. There are 35 species in the gas phase, this paper focuses on ozone concentration. The wind fields are interpolated from observed data via the method described in Goodin et al. (1979) with a divergence criterion to be less than  $10^{-3} \, \mathrm{s}^{-1}$ . In this model run, Forester filters (Forester, 1977) were used to suppress negative mass produced by ASD and GLK. No filters are used with QSTSE.

### 4. Results

To measure the relative accuracy among the algorithms, the following performance indices are evaluated:

$$MC = \frac{\sum_{x,y} c(x, y, t)}{\sum_{x,y} c(x, y, 0)},$$
 (23)

$$MD = \frac{\sum_{x,y} c(x, y, t)^2}{\sum_{x,y} c(x, y, 0)^2},$$
(24)

MA = 
$$\frac{\text{Max}[c(x, y, t)]}{100}$$
, (25)

$$MI = \frac{Min[c(x, y, t) - 10.0]}{100},$$
(26)

$$ME = \frac{Max|c(x, y, t) - c_{exact}(x, y, t)|}{100}.$$
 (27)

MC, MD, MA, MI, and ME are the mass conservation ratio, mass distribution ratio, maximum concentration

ratio, minimum concentration ratio, and maximum error ratio, respectively.

Fig. 1 shows the result of QSTSE for test case I, the rotating cosine hill. After two revolutions the maximum peak of 100 is maintained closely with QSTSE. Table 1 summarizes the results of the schemes after two revolutions of the cosine hill. ASD and QSTSE retain their maximum peak values within 5%, but other schemes deteriorate. Concentrations that are below the background level of 10 is kept to a minimum with ASD, QSTSE, and NFCSTSE methods, but is substantial with the GLK, NFQSTSE2, and BOTT4. Mass conservation is well preserved for all schemes with QSTSE and BOTT4 preserving mass conservation exactly.

The computational times for these schemes vary substantially and are reported in Table 1. Normalizing the GLK scheme to consume 1 time unit, QSTSE, BOTT4 and ASD consume 5.8, 2.3 and 40.7 time units, respectively. These times are computed on a sequential machine with compiler optimization. The computational cost of QSTSE is not substantially more than that of NFQSTSE or NFQSTSE2, but has better performance characteristics than both of these low-order schemes.

The results of test II are presented in Figs. 2 and 3. Fig. 2 shows the performance of the schemes under rugged conditions with no spacing between the two square waves. Exact mass conservation and positive definiteness is achieved by both QSTSE and BOTT4. ASD and GLK accrued 2 and 8% mass, respectively. ASD and QSTSE are able to resolve some separation between the two square waves, while BOTT4 and GLK lumped the two square waves together. ASD overshoots the height while all other schemes underpredicts the height in this test. With a spacing of one grid point between the square waves, the various schemes perform better than without any spacing as shown in Fig. 3. QSTSE and BOTT4 are positive definite and strictly mass conservative while the others are not. With the increased spacing, all schemes exhibit some separation between the two square waves as it advects downwind. The best separation is maintained by ASD but has some serious under and over predictions. QSTSE is able to resolve the separation in addition to a height increase closer to the exact solution. Further tests conducted (not shown) with more spacing between the two square waves show performance increase in all schemes as the spacing increases.

Test III is designed primarily to gauge mass conservation among the schemes as a sharp spike passes through a divergent wind field. Fig. 4 presents the results from that test. The exact solution is derived from a Lagrangian approach. In essence, the spike located at grid point 5 broadens when it passes a velocity ramp. The exact solution is a spike near grid point 23 with a height of 0.5 and a base of radius 2. Both QSTSE and BOTT4 are exactly mass conservative and positive definite. However, ASD and GLK accrued 36% and 6% mass, respectively.

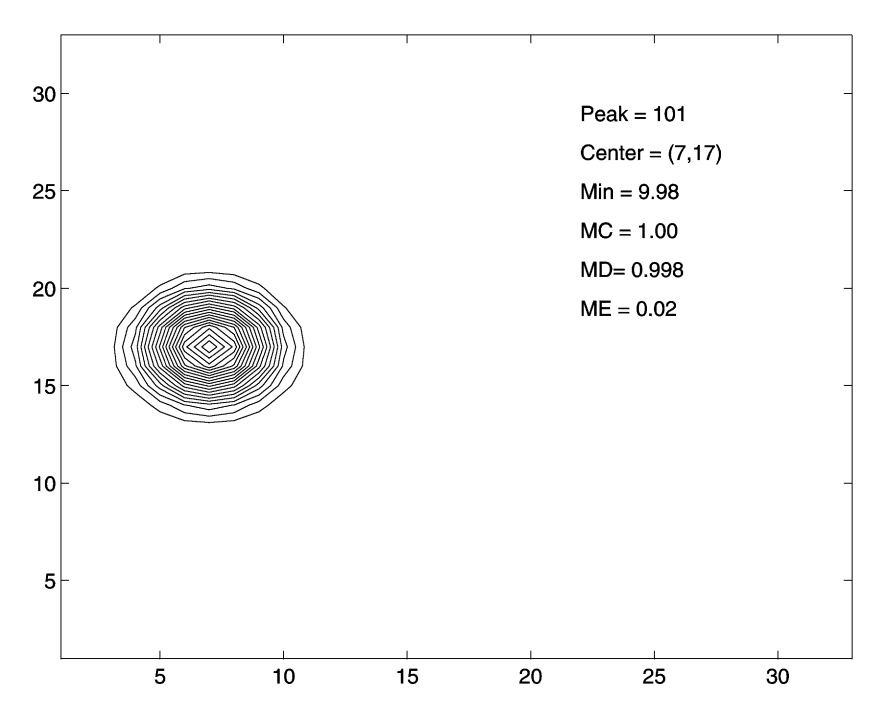


Fig. 1. Concentration profile of the rotating cosine hill advected by QSTSE for two revolutions at  $\Delta t = 30\pi$ . The peak and form of the cosine hill is preserved almost identically. The 20 contours are equally spaced contours from -2 to 100.

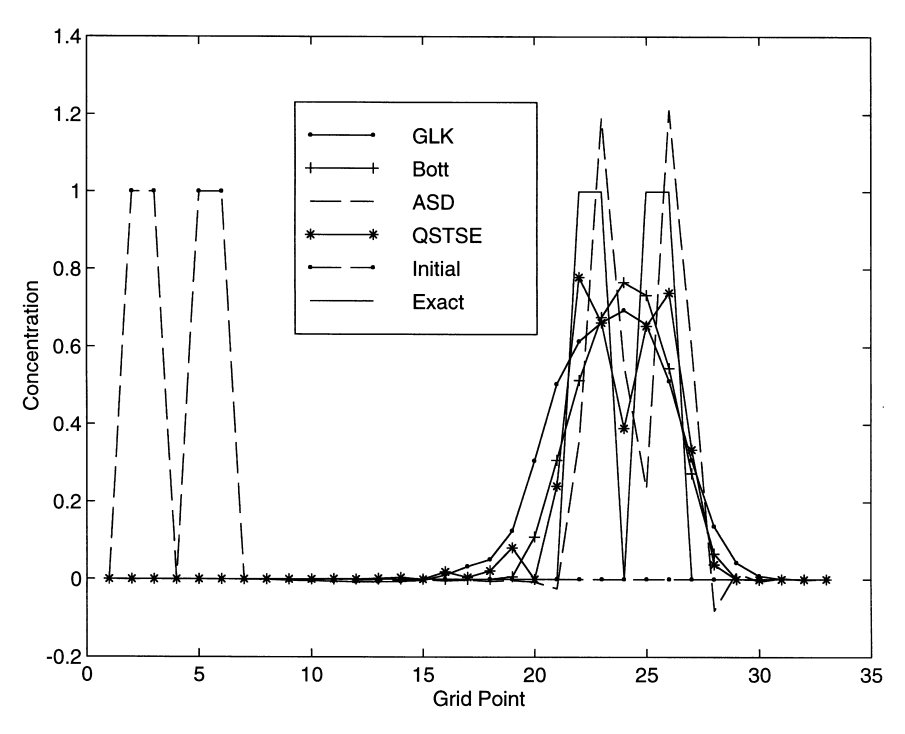


Fig. 2. Concentration profile of Test II with rugged concentration profile. There is no grid spacing between the two square waves as it is advected downwind.

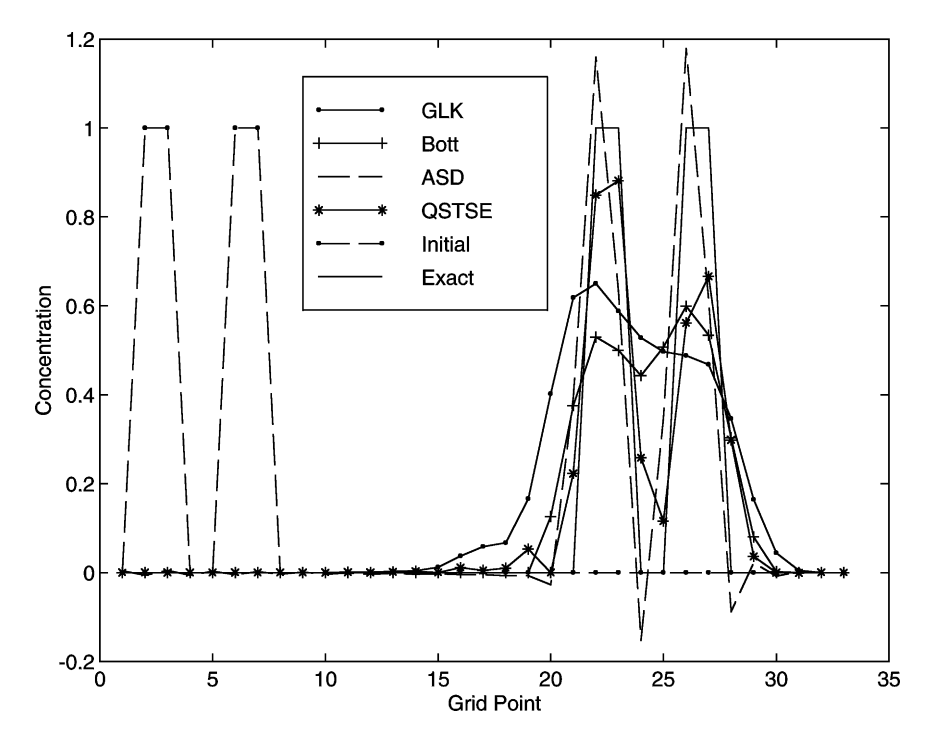


Fig. 3. Similar to Fig. 2 with the two square waves separated with one grid spacing. As the spacing increase all schemes perform better.

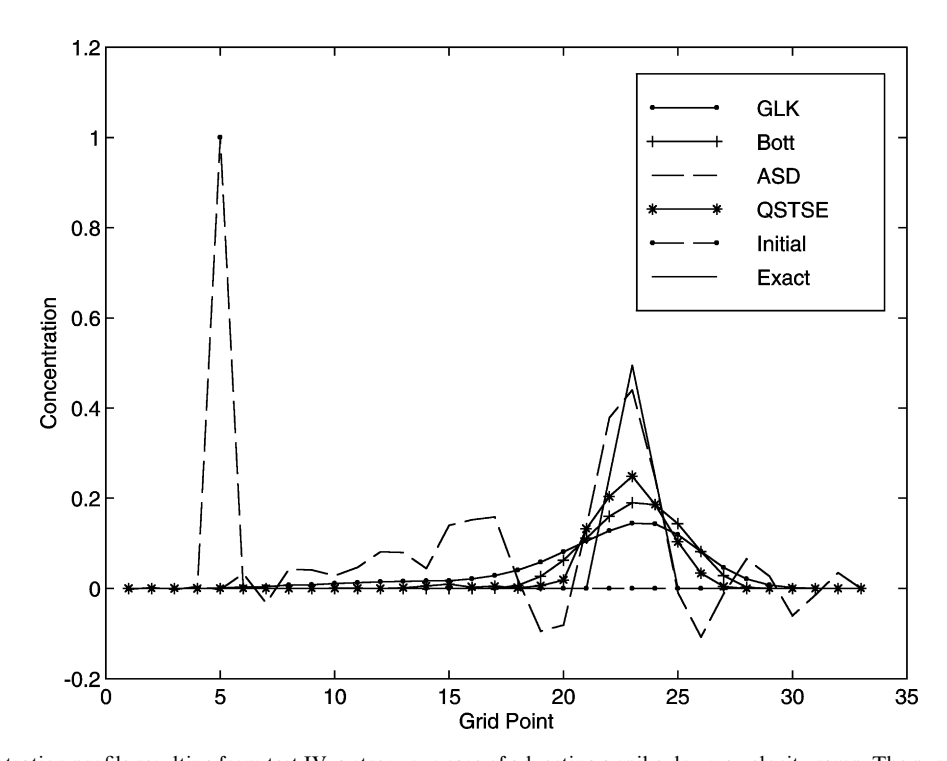


Fig. 4. Concentration profile resulting from test IV, a strenuous case of advecting a spike down a velocity ramp. The purpose of this test is measuring mass conservation.

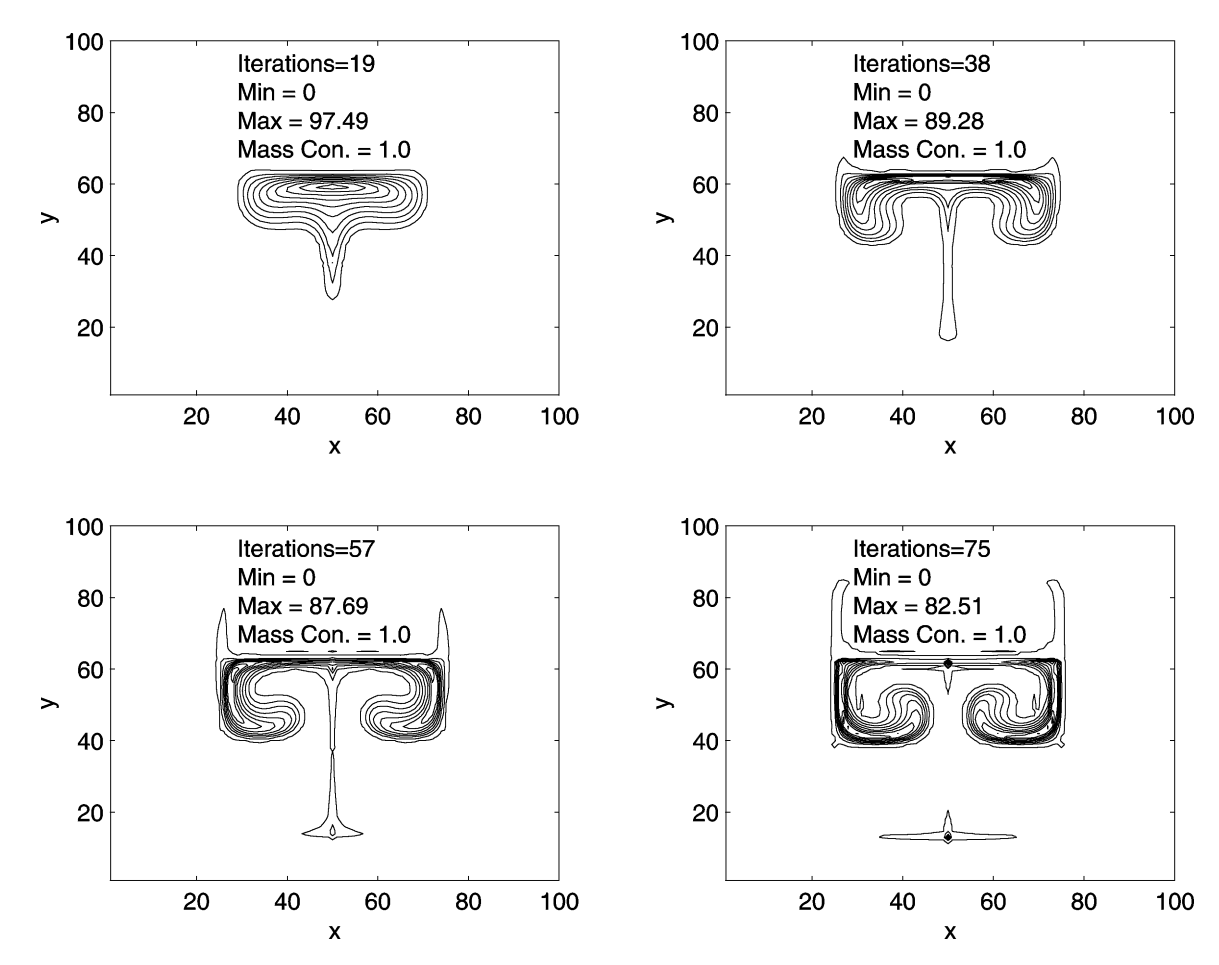


Fig. 5. Concentration profile as computed by QSTSE for the deformative flow of Smolarkiewicz (1982) after 19, 38, 57, and 75 iterations, respectively. Contours are shown at concentrations of 1, 10, 20, 30, 40, 50, 60, 70, 80, 90 and 100.

ASD predicts the peak most accurately but suffers from substantial oscillations. QSTSE, GLK and BOTT4 underpredict the peak but QSTSE retains the peak and its location better than GLK and BOTT4.

QSTSE concentration profiles for test case IV are shown in Fig. 5. The exact solution to this problem is presented in Staniforth et al. (1987). Comparing the graphs of the exact solution to the numerical one shows QSTSE's ability to retain both peak and shape under a deformative flow. Furthermore, Fig. 5 and numerical data show QSTSE's ability to preserve symmetry over the reported time increments as performed also by Bott (1989). The maximum error occured at the peak where the results of QSTSE reports 82.51 instead of 100.

Results from the full model implementation are shown in Fig. 6. The model run was made to compare QSTSE, ASD, and GLK. ASD is selected because of its accuracy and GLK its wide use and efficiency. Fig. 6 shows the measured ozone concentrations for the city of

Claremont, a location with high concentration of ozone. All schemes present similar qualitative results for ozone concentrations at Claremont. Ozone contours throughout all the simulation hours confirm this similarity between the three schemes. Results produced by ASD and QSTSE are almost identical and are closer to the observed data than results produced by GLK. In general, GLK tends to underestimate ozone concentration during the late afternoon. As described previously, the time requirements among the solvers differs by a factor of 40 in pure advection test cases. However, in a full model run the overall computational time when using different schemes differs only by a factor of 4 since the chemistry computations consume most of the CPU time. In particular, the time required by GLK and QSTSE is approximately equal. On the other hand, a full model run the ASD is approximately 4 times slower. Given that GLK took 1 time unit to complete the full model run, QSTSE and ASD consumed 1.02 and 3.95 time units, respectively.

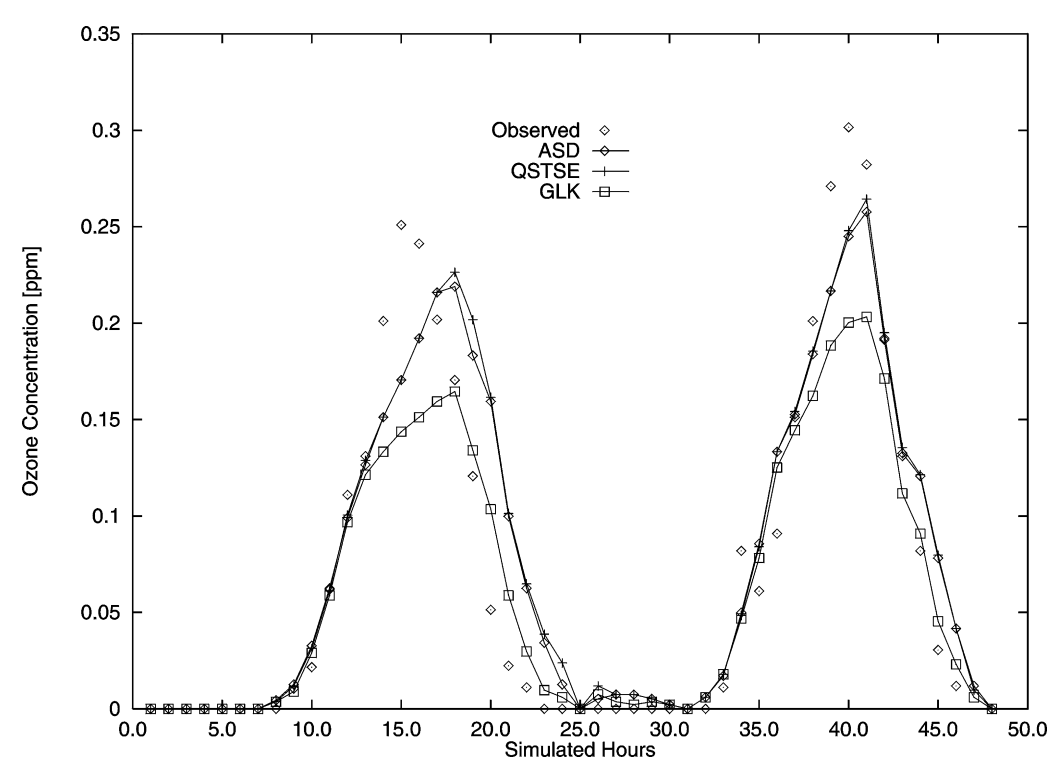


Fig. 6. Ozone concentrations at the city of Claremont as simulated by the CIT Airshed Model for 27 and 28 August of 1987. Both ASD and QSTSE predict less diffusive ozone concentrations that are closer to the observed data than those predicted by GLK.

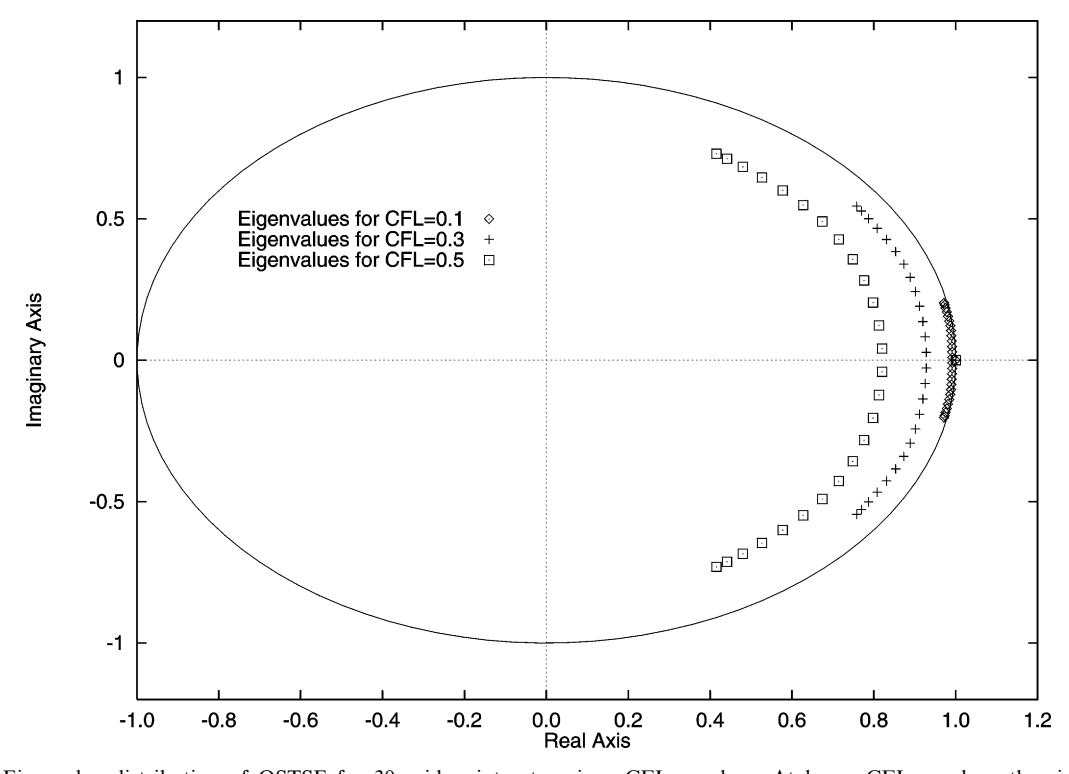


Fig. 7. Eigenvalue distribution of QSTSE for 30 grid points at various CFL numbers. At lower CFL numbers the eigenvalue distribution indicates excellent amplitude and phase preservation.

### 5. Conclusion

The advection equation plays a dominant role in air quality models. The inherent non-linearity of the chemistry operator emphasizes the importance of an accurate advection solver (Hôv et al., 1989). One of the most accurate advection solvers for air quality models reported in the literature is the accurate space derivative (ASD) method (Chock, 1991; Dabdub and Seinfeld, 1994). However, it is computational expensive and requires extraneous periodic boundary conditions. In this paper, quintic spline interpolation techniques are used to solve the advection equation. The new scheme, QSTSE, is significantly faster and produces similar peak retention properties than ASD in classical test cases while maintaining both positive definiteness and exact mass conservation. In a full model run, ASD and QSTSE produce nearly identical results. QSTSE is slightly slower than the Taylor-Galrerkin scheme (currently implemented), Taylor-Galerkin (GLK). However, the increased accuracy of OSTSE over GLK improves predicted peak ozone concentrations in a full model simulation by 27.5%.

### Acknowledgements

This project has been funded in part with Federal Funds from Environmental Protection Agency under a Grant No. R 826371-01-0 and the Earth Systems Science thrust area of the National Partnership for Advanced Computational Infrastructure. The results and content of this publication do not reflect necessarily, the views and opinions of the Agency or the US Government.

### Appendix A

The classical eigenvalue analysis on stability by the matrix method (Hirsch, 1990) provides useful information of the behavior the NFQSTSE. The eigenvalue stability of the NFQSTSE is applied on the model equation (Hirsch, 1990),

$$\frac{\partial c}{\partial t} = -\gamma \frac{\partial c}{\partial x},\tag{A.1}$$

where  $\gamma$  is a constant speed.

In order to apply the matrix stability method, the solution to Eqs. (3)–(7) should be cast in matrix form

$$b = Ba, (A.2)$$

$$c = \frac{Ca}{2},\tag{A.3}$$

$$d = \frac{Da}{6},\tag{A.4}$$

$$e = \frac{Ea}{24},\tag{A.5}$$

$$f = \frac{Fa}{120},\tag{A.6}$$

where B, C, D, E, F are the matrix operators that computes the coefficients of the quintic spline. With the coefficients represented in matrix form, the advancement of the solution to Eq. (A.1) by the algorithm described in Section 2.1 is given as

$$c^{n+1} = \left(I - \Delta t \gamma B + \frac{\Delta t^2}{2!} \gamma^2 C - \frac{\Delta t^3}{3!} \gamma^3 D + \frac{\Delta t^4 \gamma^4 E}{4!} \right) c^n,$$
(A.7)

where  $c^n$  is the nodal value of the concentration at time step n. The eigenvalues of the matrix,

$$S = \left(I - \Delta t \gamma B + \frac{\Delta t^2}{2!} \gamma^2 C - \frac{\Delta t^3}{3!} \gamma^3 D + \frac{\Delta t^4 \gamma^4 E}{4!}\right), \quad (A.8)$$

detail the stability behavior of NFQSTSE. The computation of the full matrix, S, depends on the number of grid points N and, thus, making the analytical eigenvalues of S elusive. Instead, the eigenvalues are obtained numerically for a wide range of CFL =  $\gamma \Delta t/\Delta x$  numbers. Stable CFL numbers are extrapolated by analyzing the graph of the spectral radius,  $\rho(S)$ , where  $\rho(S) \leq 1$ . From the results obtained, the CFL stability criterion for the NFQSTSE is satisfied providing that

$$CFL < 1.0. (A.9)$$

Fig. 7 presents eigenvalue distributions of the NFQSTSE with N=30 points for CFL = 0.1, 0.3, and 0.5. At lower CFL numbers the NFQSTSE is able to transport the signal effectively without much damping or dispersion as indicated with the eigenvalues near 1.0. As CFL increases the eigenvalues spread out inside the stability circle and is expected to dampen the signal, as do most solvers.

### References

Augenbaum, J.M., 1984. A Lagrangian method for the shallowwater equations on a Voronoi mesh. Journal of Computational Physics 53, 240–265.

Bermejo, R., Staniforth, A., 1992. The conversion of semi-Lagrangian advection schemes to quasi-monotone schemes. Monthly Weather Review 120, 2622–2632.

Bott, A., 1989. A positive definite advection scheme obtained by nonlinear renormalization of the advective fluxes. Monthly Weather Review 117, 1006–1015.

Chock, D.P., 1985. A comparison of numerical methods for solving the advection equation-II. Atmospheric Environment 19, 571–586.

Chock, D.P., 1991. A comparison of numerical methods for solving the advection equation-III. Atmospheric Environment 25A, 853-871.

- Chock, D.P., Dunker, A.M., 1983. A comparison of numerical methods for solving the advection equation. Atmospheric Environment 17, 11–24.
- Chock, D.P., Sun, P., Winkler, S.L., 1996. Trajectory-grid an accurate sign-preserving advection-diffusion approach for air quality modeling. Atmospheric Environment 30, 857–868
- Costantini, P., 1986. On monotone and convex spline interpolation. Mathematics of Computation 46, 203–214.
- Costantini, P., 1988. An algorithm for computing shape-preserving interpolating splines of arbitrary degree. Journal of Compututational and Applied Mathematics 22, 89–136.
- Dabdub, D., Seinfeld, J.H., 1994. Numerical advection schemes used in Air Quality Models-sequential and parallel implementation. Atmospheric Environment 28, 3369–3385.
- De Boor, C., 1978. A Practical Guide to Splines. Springer, New York
- Dhaniyala, S., Wexler, A., 1996. Numerical schemes to model condensation and evaporation of aerosols. Atmospheric Environment 30, 919–928.
- Dubeau, F., Savoie, J., 1983. Periodic quadratic spline interpolation. Journal of Approximation Theory 39, 77–88.
- Fischer, B., Opfer, G., Puri, M.L., 1991. A local algorithm for constructing non-negative cubic splines. J. Approx. Theory 64, 1-16.
- Forester, C.K., 1977. Higher order monotonic convective difference schemes. Journal of Computational Physics 23, 1–22.
- Gazdag, J., 1973. Numerical convective schemes based on accurate computation of space derivatives. Journal of Computational Physics 13, 100–113.
- Goodin, W.R., McRae, G.J., Seinfeld, J.H., 1979. An objective analysis of technique for constructing three-dimensional urban-scale wind fields. Journal of Applied Meteorology 19, 96–106.
- Harley, R.A., Russell, A.G., McRae, G.J., Cass, G.R., Seinfeld, J.H., 1993. Photochemical modeling of the Southern California air quality study. Environmental Science and Technology 27, 378–388.
- Hirsch, C.A., 1990. Numerical Computation of Internal and External Flows. Wiley, New York.

- Hôv, O., Zlatev, Z., Berkowicz, R., Eliassen, A., Prahm, L.P., 1989. Comparison of numerical techniques for use in air pollution models with nonlinear chemical reactions. Atmospheric Environment 23, 967–983.
- Huang, C.Y., 1996. A comparative study of high-order, quasiconservative, Semi-Lagrangian, and Eulerian advection schemes. Journal of Applied Meteorology 36, 599–613.
- McAllister, D.F., Passow, E., Roulier, J.A., 1977. Algorithms for computing shape preserving spline interpolations to data. Mathematics of Computation 31, 717–725.
- Oran, E.S., Boris, J.P., 1987. Numerical Simulation of Reactive Flow. Elsevier, New York.
- Pepper, D.W., Long, P.E., 1978. A comparison of results using second-order moments with and without width correction to solve the advection equation. Journal of Applied Meteorology 17, 228–233.
- Purnell, D.K., 1976. Solution of the advection equation by upstream interpolation with cubic splines. Monthly Weather Review 104, 42–48.
- Rood, R.B., 1987. Numerical advection algorithms and their role in atmospheric transport and chemistry models. Reviews of Geophysics 24, 71–100.
- Schmidt, J.W., Hess, W., 1988. Positivity of cubic polynomials on intervals and positive spline interpolation. BIT 28, 340-352.
- Schoenberg, I.J., 1983. Splines and histograms. Spline Functions and Approximation Theory, Proceedings of the Symposium, University of Alberta, Edmonton. ISNM 21, Basel, Switzerland.
- Smolarkiewicz, P.K., 1982. The multidimensional Crowley advection scheme. Monthly Weather Review 110, 1968–1983.
- Spath, H., 1995. One Dimensional Spline Interpolation Algorithms. Addison-Wesley, Reading, MA.
- Spath, H., Meier, J., 1988. Flexible smoothing with periodic cubic splines and fitting with closed curves. Computing 40, 293–300.
- Staniforth, A., Cote, J., Pudykiewicz, J., 1987. Comments on Smolarkiewicz's deformational flow. Monthly Weather Review 115, 894–900.
- Yanenko, N.N., 1971. The Method of Fractional Steps. Springer, New York.